Residual Plaque Burden, Delivered Dose, and Tissue Composition Predict 6-Month Outcome After Balloon Angioplasty and ß-Radiation Therapy

Manel Sabaté, Johannes P. A. Marijnissen, Stéphane G. Carlier, I. Patrick Kay, Willem J. van der Giessen, Veronique L. M. A. Coen, Jurgen M. R. Ligthart, Eric Boersma, Marco A. Costa, Peter C. Levendag and Patrick W. Serruys

Circulation 2000;101;2472-2477
Circulation is published by the American Heart Association. 7272 Greenville Avenue, Dallas, TX 72514
 Print ISSN: 0009-7322. Online ISSN: 1524-4539

Residual Plaque Burden, Delivered Dose, and Tissue Composition Predict 6-Month Outcome After Balloon Angioplasty and β-Radiation Therapy

Manel Sabaté, MD; Johannes P.A. Marijnissen, PhD; Stéphane G. Carlier, MD; I. Patrick Kay, MBChB; Willem J. van der Giessen, MD, PhD; Veronique L.M.A. Coen, MD; Jurgen M.R. Ligthart, BSc; Eric Boersma, PhD; Marco A. Costa, MD; Peter C. Levendag, MD, PhD; Patrick W. Serruys, MD, PhD

Background—Inhomogeneity of dose distribution and anatomic aspects of the atherosclerotic plaque may influence the outcome of irradiated lesions after balloon angioplasty (BA). We evaluated the influence of delivered dose and morphological characteristics of coronary stenoses treated with β-radiation after BA.

Methods and Results—Eighteen consecutive patients treated according to the Beta Energy Restenosis Trial 1.5 were included in the study. The site of angioplasty was irradiated with the use of a β-emitting $^{90}Sr/^{90}Y$ source. With the side branches used as anatomic landmarks, the irradiated area was identified and volumetric assessment was performed by 3D intracoronary ultrasound imaging after treatment and at 6 months. The type of tissue, the presence of dissection, and the vessel volumes were assessed every 2 mm within the irradiated area. The minimal dose absorbed by 90% of the adventitial volume (D_{v90}Adv) was calculated in each 2-mm segment. Diffuse calcified subsegments and those containing side branches were excluded. Two hundred six coronary subsegments were studied. Of those, 55 were defined as soft, 129 as hard, and 22 as normal/intimal thickening. Plaque volume showed less increase in hard segments as compared with soft and normal/intimal thickening segments ($P<0.0001$). D_{v90}Adv was associated with plaque volume at follow-up after a polynomial equation with linear and nonlinear components ($r=0.71$; $P=0.0001$). The multivariate regression analysis identified the independent predictors of the plaque volume at follow-up: plaque volume after treatment, D_{v90}Adv, and type of plaque.

Conclusions—Residual plaque burden, delivered dose, and tissue composition play a fundamental role in the volumetric outcome at 6-month follow-up after β-radiation therapy and BA. **(*Circulation*. 2000;101:2472-2477.)**

Key Words: balloon ■ angioplasty ■ radioisotopes ■ ultrasonics ■ restenosis

Endovascular radiation therapy is a promising new technique aimed at preventing restenosis after percutaneous coronary intervention.[1–3] Although its effectiveness has been proven in the treatment of in-stent restenosis,[4] the value of intracoronary irradiation in de novo coronary lesions remains to be established. Radiation delivered to the coronary artery by means of catheter-based systems can use both γ- and β-emitters.[5] Long-term results after treatment may be influenced by absolute dose and by the homogeneity in dose distribution. β-Emitters demonstrate a more rapid dose fall-off than γ-emitters because of the short range of electrons.[6] This feature may lead to a less homogeneous dose distribution when treating coronary segments with variable degrees of curvature, tapering, remodeling, and plaque extent. The use of dose-volume histograms allows one to evaluate the cumulative dose received by a certain specified tissue volume[7] and has been recently implemented in the field of intracoronary brachytherapy as a tool for dosimetry.[8] Aims of the study were (1) to determine, by the use of dose-volume histograms, the dose distribution of the β-emitter $^{90}Sr/^{90}Y$ along the coronary irradiated segment when delivered by a noncentered device, (2) to establish the dose that could be predictive of efficacy in intracoronary brachytherapy, and (3) to determine the intravascular ultrasound (IVUS) predictors of the plaque volume at 6-month follow-up of coronary segments treated with balloon angioplasty (BA) followed by β-radiation therapy.

Methods

Patient Selection

Eighteen consecutive patients with single de novo coronary stenosis successfully treated with BA followed by intracoronary β-radiation

Received September 22, 1999; revision received November 23, 1999; accepted December 22, 1999.

From the Thoraxcenter, Heartcenter, Rotterdam, Dijkzigt Academisch Ziekenhuis Rotterdam, The Netherlands (M.S., S.G.C., I.P.K., W.J.v.d.G., J.M.R.L., E.B., M.A.C., P.W.S.), and Daniel den Hoed Cancer Center, Rotterdam, The Netherlands (J.P.A.M., V.L.M.A.C., P.C.L.).

Correspondence to Prof P.W. Serruys, MD, PhD, Heartcenter, Academisch Ziekenhuis Rotterdam, Erasmus University, Bd 418, PO Box 2040, Dr Molewaterplein 40, 3015 GD Rotterdam, The Netherlands. E-mail serruys@card.azr.nl

Circulation **is available at http://www.circulationaha.org**

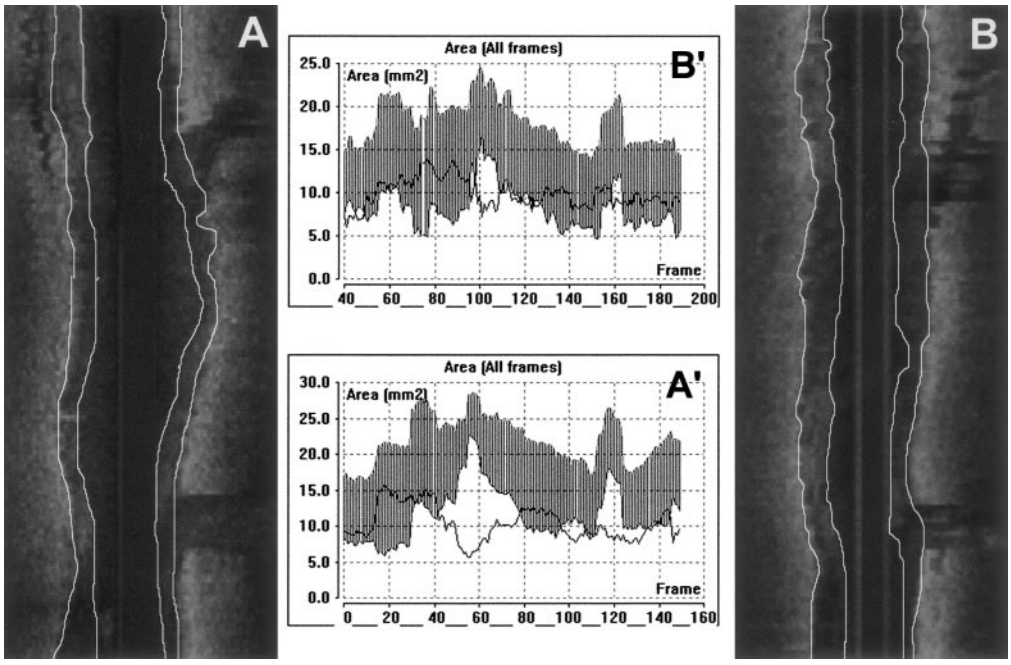

Figure 1. Longitudinal reconstruction and volumetric calculations (charts) of irradiated coronary segments after treatment (A and A′) and at 6-month follow-up (B and B′).

therapy were included in the study. Patients receiving a stent were excluded from the analysis. β-Radiation was delivered according to the Beta Energy Restenosis Trial 1.5. The isotope selected was the pure β-emitting $^{90}Sr/^{90}Y$, and patients were randomly assigned to receive 12, 14, or 16 Gy at 2 mm from the source axis. The inclusion and exclusion criteria of this trial have been previously reported.[9] The delivery of the radiation was performed by the use of the Beta-Cath System (Novoste Corp).[10] The radiation source train of this system consists of a series of 12 independent 2.5-mm-long cylindrical seeds that contain the $^{90}Sr/^{90}Y$ sources and is bordered by 2 gold radiopaque markers at distal and proximal parts separated by 30 mm.[10]

IVUS Analysis

The treated coronary segment was evaluated by means of 3D IVUS imaging, which allowed volumetric calculations of the irradiated area. The selection of the area of interest has been reported elsewhere.[11] In brief, a few steps were followed: First, an angiogram was performed after positioning the delivery catheter and the relation between anatomic landmarks and the 2 gold markers were documented. The anatomic landmark closest to either of the gold markers was used as a reference point. This angiographic reference point was identified during a contrast injection with the IVUS imaging element at the same position as the gold marker of the source. The image from the IVUS imaging element was recorded and the reference point identified. During the subsequent pullback, this reference point was recognized and used for selecting the area subject to the analysis: 30 mm for the irradiated segment.[12] The system used for imaging was a mechanical IVUS system (ClearView, CVIS, Boston Scientific Corp) with a sheath-based IVUS catheter incorporating a 30-MHz, single-element transducer rotating at 1800 rpm (Ultracross, CVIS). The transducer is placed inside a 2.9F, 15-cm-long sonolucent distal sheath that alternatively houses the guide wire (during the catheter introduction) or the transducer (during imaging). The IVUS transducer was withdrawn through the stationary imaging sheath by an ECG-triggered pullback device with a stepping motor.[12] The ECG-gated image acquisition and digitization was performed by a workstation designed for the 3D reconstruction of echocardiographic images[12] (EchoScan, Tomtec). Description of this system has been previously reported in detail.[12–14] In brief, the steering logic of the workstation considered the heart rate variability and only acquired images from cycles meeting a predetermined range and coinciding with the peak of the R wave. If an R-R interval failed to meet the preset range, the IVUS catheter remained at the same site until a cardiac cycle met the predetermined R-R range. The IVUS transducer then was withdrawn 0.2 mm to acquire the next image.[12–14] This system ensures the segment-to-segment independence by avoiding taking images during the axial movement of the IVUS catheter that occurs during the cardiac cycle. Given the slice thickness of 0.2 mm and the length subject to the analysis of 30 mm (distance between the 2 gold markers of the radiation source), 150 cross-sectional images per segment were digitized and analyzed. A semiautomatic contour detection program was used for the 3D analysis.[15] This program constructs 2 longitudinal sections from the data set and identifies the contours corresponding to the lumen-intima and media-adventitia boundaries. Corrections could be performed interactively by "forcing" the contour through visually identified points; the entire data set then was updated.[15] Careful checking and editing of the contours of the 150 planar images was performed with an average of 45 minutes for complete evaluation. The area encompassed by the lumen-intima and media-adventitia boundaries defined the luminal and the total vessel volumes, respectively. The difference between total vessel and luminal volumes defined the plaque volume. Because media thickness cannot be measured accurately, we assumed that the plaque volume included the atherosclerotic plaque and the media.[16] Volumetric data were calculated by the formula $V=\Sigma^{n}_{i=1}A_i \cdot H$, where V=volume, A=area of total vessel or lumen or plaque in a given cross-sectional ultrasound image, H=thickness of the coronary artery slice that is reported by this digitized cross-sectional IVUS image, and n=the number of digitized cross-sectional images encompassing the volume to be measured.[15] At follow-up, meticulous matching of the region of interest was performed by comparing the longitudinal reconstruction with that after treatment as previously described[11] (Figure 1). The feasibility and intraobserver and interobserver variability of this system have been previously reported.[11,13,17,18] For the purposes of the study, the computed volume of the irradiated segment was divided into 2-mm-long subsegments. Since the irradiated segment measured 30 mm, 15 subsegments were defined per patient, each of them with 10 IVUS cross sections (0.2 mm per cross section). All individual cross sections were studied by 2 investigators, blinded to the dosimetry results. Type of plaque and the

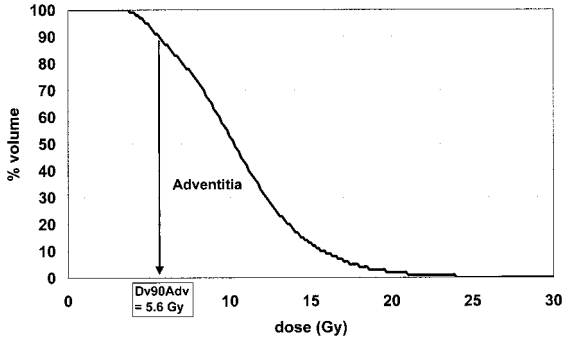

Figure 2. Dose-volume histogram showing cumulative dose received at level of adventitial layer. Minimal dose received by 90% of adventitial volume (D_{v90}Adv) is calculated.

presence of dissection were qualitatively assessed. Type of plaque was defined in every cross section as intimal thickening, soft, fibrous, mixed, and diffuse calcified according to the guidelines previously reported.[19] Intimal thickening was defined when the thickness of the intima-media complex was <0.3 mm.[19] Soft tissue was defined when ≥80% of the cross-sectional area was constituted by material showing less echoreflectivity than the adventitia, with an arc of calcium <10°, fibrous plaque when the echoreflectivity of ≥80% of the material was as bright as or brighter than the adventitia without acoustic shadowing, diffuse calcified plaque when it contained material brighter than the adventitia showing acoustic shadowing in >90°, and mixed when the plaque did not match the 80% criterion.[19] We categorized the 2-mm-long subsegments as normal/intimal thickening, soft, hard (fibrous and mixed), and diffuse calcified when ≥80% of the cross sections within the subsegment were of the same type. In those cross sections containing up to 90° of calcium arc, the contour of the external elastic membrane was imputed from noncalcified slices. Dissection of the vessel was defined as a tear parallel to the vessel wall.[19] Changes in luminal, plaque, and total vessel volume between immediately after treatment and at follow-up were also computed per subsegment. Those subsegments in which the origin of side branches involved >90° of the circumferential arc in >50% of the cross sections or were defined as diffuse calcified were excluded from the analysis.

Dose Calculation

The actual dose received by the vessel was retrospectively calculated by means of dose-volume histograms[7] in every 2-mm-long subsegment. This method is based on quantitative IVUS under the assumption that the radiation source is positioned at the same place as the IVUS catheter.[8] The distance between the center of the catheter and media-adventitia interface was calculated in 24 pie slices (15°) in all cross sections corresponding to the irradiated area.[9] Considering the prescribed dose and the accurate geometric data obtained from the IVUS, the cumulative curve of the dose-volume histogram for a predefined volume (ie, adventitia as calculated at 0.5 mm outside the external elastic membrane) can be obtained (Figure 2). From this curve, the minimum dose received by 90% of the adventitial volume (D_{v90}Adv) was calculated. The methodology and feasibility of this dosimetry approach in vascular brachytherapy has been previously reported.[8]

Statistical Analysis

Data are presented as mean±SD or proportions. Differences in quantitative IVUS data between the types of tissue were assessed by means of 1-way ANOVA. Differences in quantitative IVUS data between subsegments with and without dissection and with and without calcium were evaluated by the use of an unpaired Student's *t* test. To determine the relation between the dose received by the adventitia and the plaque volume at follow-up, linear regression analysis was performed first. Then, nonlinear components were added to the equation (x^{-1} and x^{-2} were added to describe the steep increase of plaque volume at low dose). These components were included in the model if they described the relation significantly better. Finally, the model was corrected for the plaque volume after treatment. Multivariable regression analyses were performed to identify independent predictors of plaque volume at follow-up among IVUS-derived (types of tissue, dissection, and plaque volume after treatment) and dosimetric variables (D_{v90}Adv). All tests were 2-tailed, and a value of $P<0.05$ was considered statistically significant.

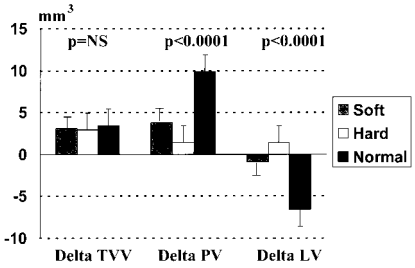

Figure 3. Changes between postprocedure and 6-month measurements in total vessel, plaque, and luminal volumes regarding different types of tissue. TVV indicates total vessel volume; PV, plaque volume; and LV, luminal volume.

Results

Baseline Characteristics

Two hundred seventy subsegments were defined in 18 patients successfully treated with BA followed by intracoronary brachytherapy. Sixty-four subsegments were excluded from the final analysis because of either diffuse calcified plaque that precluded the quantification of the total vessel volume (n=30) or side branches that involved >90° of the circumferential arc in >50% of the cross sections (n=34). Therefore, 206 irradiated subsegments were the subject of the study. Fifty-five (27%) subsegments were defined as soft, 129 (62%) as hard, and 22 (11%) as normal/intimal thickening. Dissection was observed in 34 (16.5%) subsegments.

Volumetric Changes and Dosimetry

On average, total vessel volume increased at follow-up (32.5±9 mm^3 after treatment to 35.5±11 mm^3 at follow-up; $P<0.0001$), accommodating a parallel increase in plaque volume (15.3±6 to 18.3±7 mm^3; $P<0.0001$). As a result, mean luminal volume remained unchanged (17.1±7 to 17.0±7 mm^3; P=NS). Subsegments with hard tissue demonstrated less increase in plaque, resulting in an increase in luminal volume as compared with soft and normal/intimal thickening subsegments (Figure 3). The behavior of those hard subsegments containing

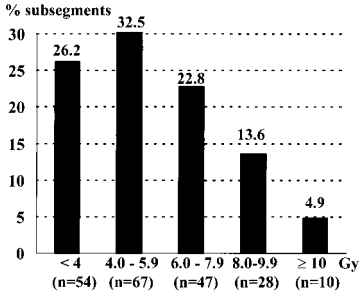

Figure 4. Range of dose distribution in irradiated coronary subsegments as calculated by dose-volume histograms.

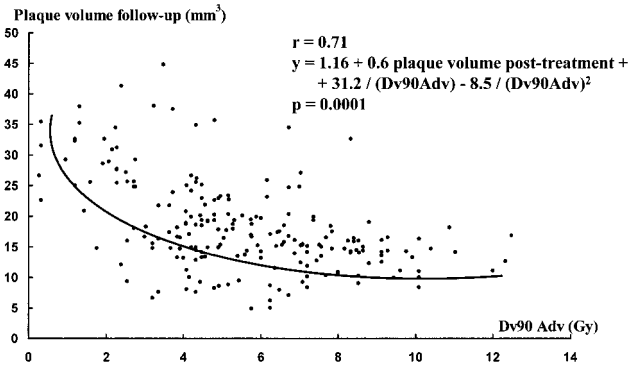

Figure 5. Relation between plaque volume at follow-up and D_{v90}Adv.

mixed calcified tissue (up to 90°; n=104) was compared with those containing mixed noncalcified tissue (n=25). Mean changes in plaque and total vessel volumes were comparable (Δplaque [mm^3]: +1.3±4.2 in mixed calcified vs +1.8±5.2 in mixed noncalcified; *P*=NS; Δtotal vessel volume [mm^3]: +2.6±6.2 in mixed calcified vs +4.2±5.8 in mixed noncalcified; *P*=NS), resulting in a comparable mean increase in luminal volume at follow-up (+1.3±5.2 mm^3 in mixed calcified vs +1.9±5.7 mm^3 in mixed noncalcified; *P*=NS). Dissected subsegments demonstrated a trend toward a smaller increase in plaque as compared with nondissected subsegments (+1.2±3 vs +3.3±6 mm^3; *P*=0.08). The mean of all 3 prescribed doses at 2 mm from the source was 14±1.8 Gy. The calculated D_{v90}Adv was 5.5±2.5 Gy (range 0.2 to 12.4). A wide range of dose distribution was observed in the irradiated coronary subsegments (Figure 4). The association between D_{v90}Adv with the plaque volume at follow-up is depicted in Figure 5. The model appeared to follow a polynomial equation with linear and nonlinear components. Nonlinear components described the increase in plaque volume at lower doses, whereas the residual plaque volume after treatment accounted for the linear relation of the curve. Changes in plaque volume appeared to decrease with dose (Figure 6). Four Gray was the minimum effective dose to be delivered to 90% of the adventitia because subsegments receiving at least this dose demonstrated a significantly smaller increase in plaque volume as compared with those receiving <4 Gy (*P*<0.001). As a result, luminal volume decreased significantly less in those subsegments receiving ≥4 Gy and even increased when the minimal dose to the adventitia was >6 Gy. Multivariable regression analyses identified plaque volume after treatment as a positive predictor of plaque volume at follow-up, whereas D_{v90}Adv and type of plaque (hard) were negative predictors (Table).

Parameters Associated With Plaque Volume at Follow-Up

	Parameter Estimate	95% CI	*P*
Plaque volume after treatment, mm^3	0.6	0.8/0.5	0.0001
D_{v90}Adv, Gy	−4.4	−5.6/−2.9	0.0001
Type of plaque (hard vs other)	−1.6	−3.4/0.1	0.06

Discussion

This study demonstrates for the first time the relation between plaque increase, as assessed by IVUS, and the dose received by the adventitia, as calculated by means of dose-volume histograms. A plot of dose-volume histogram is a standard method used in radiotherapy that condenses the large body of information available from conventional 3D distribution data

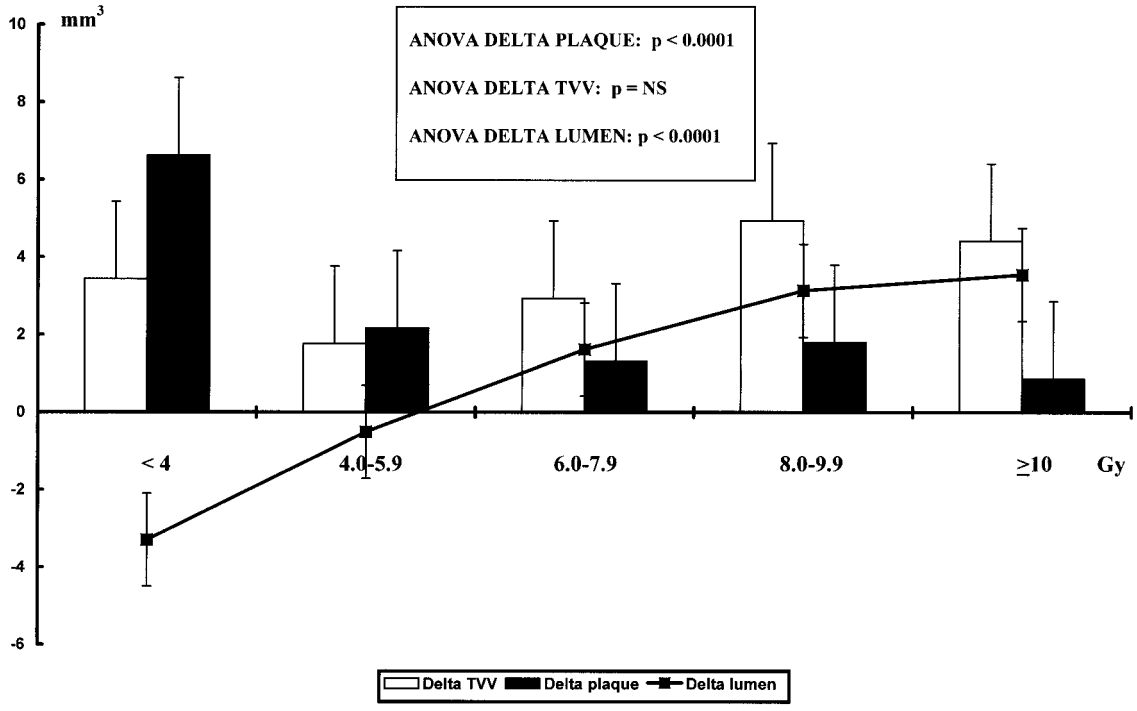

Figure 6. Changes in total vessel, plaque, and luminal volumes regarding 5 ranges of doses as calculated by dose-volume histograms. TVV indicates total vessel volume.

into a plot summarizing graphically the radiation distribution throughout the target volume.[7]

The assumption of the adventitia as the target tissue is supported by experimental studies.[20,21] Scott et al[20] localized the proliferating cells in the adventitia and their migration into the neointima after angioplasty by using bromodeoxyuridine immunohistochemistry. Similarly, Waksman et al[21] demonstrated a greater cell proliferation in control vessels 3 days after angioplasty in the adventitia at the site of the medial tear as compared with the medial wall in the same region. In this study, the proliferation was significantly reduced in irradiated vessels with either a source of $^{90}Sr/^{90}Y$ or ^{192}Ir that delivered 14 or 28 Gy at 2 mm into the artery wall.[21]

The actual dose received by the adventitia appeared to be rather low as compared with the prescribed dose at 2 mm from the source. Furthermore, the dose varied considerably between coronary subsegments, as demonstrated by the dose distribution depicted in the Figure 4. The use of β-radiation may account in part for this dose inhomogeneity. As compared with γ-radiation, β-sources have more fall-off because of the short range of electrons.[6] This feature may become crucial when treating vessels with a great degree of vessel tapering or, alternatively, lesions showing positive remodeling where the distance from the source to the surrounding adventitia may be smaller or greater than expected. In this regard, the use of IVUS as a tool for dosimetry in β-radiation therapy may become mandatory.

Dose uniformity also may be influenced by the source centering in the lumen.[22] By the use of dose-volume histograms, Carlier et al[8] demonstrated in 10 patients treated with balloon angioplasty followed by intracoronary β-radiation that the prescribed dose was administered in only 35% of the adventitia. After centering the source in the lumen, up to 60% of the adventitia may have received this dose.

The remnant plaque burden at the site of angioplasty becomes a powerful predictor of the outcome. This is in accordance with other studies that identified, either in nonstented or stented coronary segments, postintervention cross-sectional area as a predictor of restenosis.[23,24] In this regard, the usefulness of a debulking technique before radiation therapy should be addressed in further studies.

D_{v90}Adv was also identified as an independent predictor of the plaque volume at follow-up. The relation between D_{v90}Adv and plaque volume at follow-up appeared to be polynomial with linear and nonlinear components. This may model the survival curve of mammalian cells.[25] The minimal effective dose to be delivered to 90% of the adventitial volume appeared to be 4 Gy. Further increase in dose resulted in net increase in luminal volume at follow-up. Similarly, in a subgroup analysis of the SCRIPPS trial, late loss was significantly lower when the entire circumference of the adventitial border was exposed to $\geq$8 Gy.[26] Radiation doses $>$20 Gy have been suggested to be able to completely eliminate the smooth muscle cell population from the treated area.[27] However, because cells from normal tissue have a limited capacity to proliferate,[28] lower doses probably would be sufficient to permanently prevent restenosis.

Finally, subsegments containing hard tissue (fibrotic and calcified material up to 90° of the circumferential arc) demonstrated a trend to be a negative predictor of plaque volume at follow-up. Hard plaque on IVUS consists of a more mature tissue with low cellularity and high content of extracellular matrix.[29,30] These features may induce either a physical barrier for migration of smooth muscle cells from the surrounding layers or a reduced capacity to proliferate when injured as compared with that of the soft tissue with a high concentration of smooth muscle cells.[29–31] Further, it is hypothesized that tissue composition may potentially exert a different degree of shielding effect on radiation and thus become less effective. However, the degree of remodeling was similar between the different types of tissue, suggesting that the effects of attenuation of radiation induced by hard material (either containing calcium up to 90° of circumferential arc or mixed noncalcified tissue) may be negligible as compared with that of soft tissue.

Study Limitations

We assumed that the IVUS and the delivery catheters were lying in the same position in the treated coronary segment. The size of the IVUS catheter is smaller (2.9F) than the brachytherapy device (5F), which is thus to some extent more centered in the lumen. Although the catheters should be on the shortest 3D path in the lumen, coronary arteries have a complex curved geometry in space and can be partially deformed by the catheters. Thus, catheters with different rigidity may occupy different positions. The development of new systems incorporating the IVUS imaging element on the delivery catheter might resolve this drawback.

During irradiation, the position of the delivery catheter inside the lumen is not fixed and may vary along the cardiac cycle because of ventricular contractions, which may lead to some degree of inhomogeneity not assumed by data derived from the static end-diastolic IVUS images.

The behavior of diffuse calcified plaques after radiotherapy has not been evaluated because the acoustic shadowing would have impeded the reliable analysis of total vessel and plaque volumes.[19]

It has not been possible to differentiate those areas that have been traumatized and irradiated from those only irradiated. Thus, no conclusions regarding the effect on radiation in irradiated but noninjured segments can be drawn. Further studies will address this problem by defining meticulously the injured and the irradiated areas either on IVUS or quantitative coronary angiography.

Finally, the dose as presented by the use of dose-volume histograms is not a direct measurement. The theoretical value obtained at the level of the adventitia is derived from the fall-off of the isotope and the geometrical data obtained from the IVUS study. The influence of the attenuation of the radiation caused by different tissue characteristics has not been taken into consideration. Future investigations should address the implementation of a dosimetry program on-line to prescribe the radiation dose in a more refined fashion.

Acknowledgments

Dr Kay was supported by The National Heart Foundation of New Zealand. The Wenckebach prize was awarded to Dr Serruys by the

Dutch Heart Foundation for brachytherapy research in the catheterization laboratory.

References

1. Waksman R, Robinson KA, Crocker IR, et al. Endovascular low-dose irradiation inhibits neointima formation after coronary artery balloon injury in swine: a possible role for radiation therapy in restenosis prevention. *Circulation*. 1995;91:1553–1559.
2. Wiederman JG, Marboe C, Amols H, et al. Intracoronary irradiation markedly reduces restenosis after balloon angioplasty in a porcine model. *J Am Coll Cardiol*. 1994;23:1491–1498.
3. Verin V, Popowski Y, Urban P, et al. Intra-arterial β-irradiation prevents neointimal hyperplasia in a hypercholesterolemic rabbit restenosis model. *Circulation*. 1995;92:2284–2290.
4. Teirstein PS, Massullo V, Jani S, et al. Catheter-based radiotherapy to inhibit restenosis after coronary stenting. *N Engl J Med*. 1997;336: 1697–1703.
5. Waksman R, ed. *Vascular Brachytherapy*. Armonk, NY: Futura Publishing Inc; 1999.
6. Amols HI. Isotopes for use in vascular brachytherapy. In: Waksman R, Serruys PW, eds. *Handbook of Vascular Brachytherapy*. London, UK: Martin Dunitz Ltd; 1998:1–4.
7. Drzymala RE, Mohan R, Brewster MS, et al. Dose-volume histograms. *Int J Radiat Oncol Biol Phys*. 1991;21:71–78.
8. Carlier SG, Marijnissen JPA, Coen VLMA, et al. Guidance of intracoronary radiation therapy based on dose-volume histograms derived from quantitative intravascular ultrasound. *IEEE Trans Med Imaging*. 1998; 17:772–778.
9. King SB III, Williams DO, Chogule P, et al. Endovascular β-radiation to reduce restenosis after coronary balloon angioplasty: results of the Beta Energy Restenosis Trial (BERT). *Circulation*. 1998;97:2025–2030.
10. Hillstead RA, Johnson CR, Weldon TD. The Beta-Cath system. In: Waksman R, Serruys PW, eds. *Handbook of Vascular Brachytherapy*. London, UK: Martin Dunitz Ltd; 1998:41–51.
11. Sabaté M, Serruys PW, van der Giessen WJ, et al. Geometric vascular remodeling after balloon angioplasty and β-radiation therapy: a 3-dimensional intravascular ultrasound study. *Circulation*. 1999;100: 1181–1188.
12. Bruining N, von Birgelen C, Di Mario C, et al. Dynamic 3-dimensional reconstruction of IVUS images based on an ECG-gated pullback device. In: *Computers in Cardiology*. Los Alamitos, Calif: IEEE Computer Society Press; 1995:633–636.
13. von Birgelen C, de Vrey EA, Mintz GS, et al. ECG-gated 3-dimensional intravascular ultrasound: feasibility and reproducibility of the automated analysis of coronary lumen and atherosclerotic plaque dimensions in humans. *Circulation*. 1997;96:2944–2952.
14. Bruining N, von Birgelen C, de Feyter PJ, et al. ECG-gated versus non-gated 3-dimensional intracoronary ultrasound analysis: implications for volumetric measurements. *Cathet Cardiovasc Diagn*. 1998;43: 254–260.
15. Li W, von Birgelen C, Di Mario C, et al. Semi-automated contour detection for volumetric quantification of intracoronary ultrasound. In: *Computers in Cardiology*. Washington, DC: IEEE Computer Society Press; 1994:277–280.
16. Mallery JA, Tobis JM, Griffith J, et al. Assessment of normal and atherosclerotic arterial wall thickness with an intravascular ultrasound imaging catheter. *Am Heart J*. 1990;119:1392–1400.
17. von Birgelen C, Di Mario C, Li W, et al. Morphometric analysis in 3-dimensional intracoronary ultrasound: an in vitro and in vivo study performed with a novel system for the contour detection of lumen and plaque. *Am Heart J*. 1996;132:516–527.
18. von Birgelen C, Mintz GS, Nicosia A, et al. Electrocardiogram-gated intravascular ultrasound image acquisition after coronary stent deployment facilitates on-line 3-dimensional reconstruction and automated lumen quantification. *J Am Coll Cardiol*. 1997;30:436–443.
19. DiMario C, Görge G, Peters R, et al. Clinical application and image interpretation in intracoronary ultrasound: study group on intracoronary imaging of the working group of coronary circulation and of the subgroup on intravascular ultrasound of the working group of echocardiography of the European Society of Cardiology. *Eur Heart J*. 1998;19:207–229.
20. Scott NA, Cipolla GD, Ross CE, et al. Identification of a potential role for the adventitia in the vascular lesion formation after balloon overstretch injury of porcine coronary arteries. *Circulation*. 1996;93:2178–2187.
21. Waksman R, Rodriguez JC, Robinson KA, et al. Effect of intravascular irradiation on cell proliferation, apoptosis and vascular remodeling after balloon overstretch injury of porcine coronary arteries. *Circulation*. 1997; 96:1944–1952.
22. Amols HI, Zaider M, Weinberger J, et al. Dosimetric considerations for catheter-based beta and gamma emitters in the therapy of neointimal hyperplasia in human coronary arteries. *Int J Radiat Oncol Biol Phys*. 1996;36:913–921.
23. Mintz GS, Popma JJ, Pichard AD, et al. Intravascular predictors of restenosis after transcatheter coronary revascularization. *J Am Coll Cardiol*. 1996;27:1678–1687.
24. Prati F, Di Mario C, Moussa I, et al. In-stent neointimal proliferation correlates with the amount of residual plaque burden outside the stent: an intravascular ultrasound study. *Circulation*. 1999;99:1011–1014.
25. Hall EJ, Miller RC, Brenner DJ. The basic radiobiology of intravascular irradiation. In: Waksman R, ed. *Vascular Brachytherapy*. 2nd ed. Armonk, NY: Futura Publishing Co Inc; 1999:63–72.
26. Teirstein PS, Massullo V, Jani S, et al. A subgroup analysis of the Scripps Coronary Radiation to Inhibit Proliferation Poststenting Trial. *Int J Radiat Oncol Biol Phys*. 1998;42:1097–1104.
27. Brenner DJ, Miller RC, Hall EJ. The radiobiology of intravascular radiation. *Int J Radiat Oncol Biol Phys*. 1996;36:805–810.
28. Fowler JF. Dose response curves for organ function or cell survival. *Br J Radiol*. 1983;56:497–500.
29. Di Mario C, The SHK, Madretsma S, et al. Detection and characterization of vascular lesions by intravascular ultrasound: an in vitro study correlated with histology. *J Am Soc Echocardiogr*. 1992;5:135–146.
30. Rasheed Q, Dhawale PJ, Anderson J, et al. Intracoronary ultrasound-defined plaque composition: computer-aided plaque characterization and correlation with histologic samples obtained during directional coronary atherectomy. *Am Heart J*. 1995;129:631–637.
31. Stary HC, Chandler AB, Dinsmore RE, et al. A definition of advanced types of atherosclerotic lesions and a histological classification of atherosclerosis: a report from the Committee on Vascular Lesions of the Council on Arteriosclerosis, American Heart Association. *Arterioscler Thromb Vasc Biol*. 1995;15:1512–1531.